CHALMERS
UNIVERSITY OF TECHNOLOGY

Environmental Assessment of Noise Abatement Approach Trajectories

33RD CONGRESS
OF THE INTERNATIONAL COUNCIL
OF THE AERONAUTICAL SCIENCES
STOCKHOLM, SWEDEN, 4-9 SEPTEMBER, 2022

ICAS 2022 SWEDEN

Environmental Assessment of Noise Abatement Approach Trajectories

Evangelia Maria Thoma[1*], Tomas Grönstedt[1], Evelyn Otero Sola[2], Xin Zhao[1]

[1]Chalmers University of Technology
[2]KTH, Royal Institute of Technology
[*]Corresponding author: marily@chalmers.se

Abstract

Noise abatement procedures are one of the main actions implemented to reduce noise pollution around airports. In this study, the focus is turned on approach operations and their environmental impact. The assessment starts from standard optimized procedures, namely the Continuous Descent Approach (CDA) and the Low Drag Low Power (LDLP) and the aim is to look into more advanced procedures, such as a Steep and a Segmented CDA, an Advanced LDLP and an optimized trajectory for the specific flight conditions. The procedures are designed for an A321neo and compared and evaluated for noise and emissions. It is demonstrated that multidisciplinary design and adaptation to specific conditions are required for the assessment of these interdependencies for flight procedures.

Keywords: Approach trajectories, noise abatement, emissions, interdependencies

1. Introduction

The environmental impact of the aviation industry has been discussed extensively in the recent years. One of the major concerns is noise and emissions around the airports. Noise from aircraft is known to cause health related problems such as heart disease and stroke while emissions have an effect both on the human health and on the climate. Progress has been achieved in the past few years concerning the reduction of noise and emissions. Efforts have focused on the aircraft-engine technology level and design, as well as the operational level and flight procedures. Most of the existing aircraft are expected to stay into service for many years, thus, it is important to explore the possibilities of noise and emissions reduction through flight path management. When focusing in areas in the vicinity of the airport, it has been established that approach noise is usually higher than the other reference points, i.e. Sideline and Cutback.

Several procedures exist aiming to limit the noise from arriving aircraft, such as Continuous Descent Approach (CDA) and Low Drag Low Power (LDLP). The main actions implemented in these procedures are increased flight altitude for the former and lower power requirement and delayed configuration changes for the latter. Another strategy, occasionally used, is the touchdown displacement. However, this requires permission and critical assessment for every flight and airport. One aspect that should be considered when designing new trajectories is that minimum noise trajectories often lead to an increase in other emissions. Any change in the selected procedure can, for example, result in increased fuel consumption. Thus, before designing new trajectories, it is important to evaluate their environmental impact both for noise and emissions. In this study several noise abatement approach procedures are examined, as well as slightly modified procedures. Empirical and semi-empirical models are used for the prediction of noise and emissions, highlighting the flexibility of the tool and its advantage when designing new procedures. A similar study on the evaluation of noise abatement approach procedures, but with respect to noise and pilot workload, has been presented by Koenig and Macke [1].

The work performed in this study aims at the evaluation of noise abatement approach trajectories for minimum environmental impact by evaluating interdependencies between noise and CO_2 as well as non-CO_2 emissions. Trajectories are constructed using available flight recorder data and theory found in public resources, such as [2] and [3]. The procedures presented by Koening and Macke [1]

are used as a reference since they have been examined for operational feasibility and workload. Noise and emissions are, then, evaluated using in-house codes based on semi-empirical models. The framework combines a trajectory generation module, an aircraft / engine performance module, noise emissions source model and gas emissions model. A case study is presented around Arlanda airport in Stockholm for the A321neo with Leap-1A engine. Furthermore, an approach trajectory optimization for the selected aircraft and airport is also presented, indicating the importance of adapting the trajectory design to the specific conditions.

2. Methodology

2.1 Flight Dynamics Model

For the present study, the 4D trajectory of the aircraft is used, consisting of three space dimensions and time. The aircraft is assumed to be a point mass and the earth flat and non-rotational. All the forces are assumed to act on the center of gravity of the aircraft and the velocity vector on the plane of symmetry of the aircraft, meaning that the sideslip angle is zero. Furthermore, ISA conditions are applied and zero wind. Throughout the trajectory design process, the horizontal flight path is kept constant, and the vertical profile and speed are modified according to the selected type of noise abatement trajectory. It is then possible to estimate the required thrust, T, the lift, L, and the drag, D, from the following system of equations.

$$\begin{cases} T\,cos(a) - D - mg\,sin(\gamma) = \dot{V}m \\ (T\,sin(\alpha) + L)\,cos(\varphi) - mgcos(\gamma) = \dot{\gamma}mV \\ (T\,sin(\alpha) + L)\,sin(\varphi) = \dot{\psi}mVcos(\gamma) \end{cases} \quad (1)$$

where V is the true airspeed, here assumed equal to the ground speed, γ is the flight path angle, ψ is the heading angle and m is the mass of the aircraft. For the final approach segment, the fuel consumption, f, is significantly small and the weight of the aircraft can therefore be assumed constant. The angle of attack, α, is assumed constant. The bank angle, φ, is calculated to fit the desired heading angle and horizontal flight path. For the present study a fixed lift-to-drag ratio, R_f, is assumed for every configuration. For the determination of R_f available data from an aircraft model were used and the values are presented in Table 1, where LG denotes a deployed landing gear. The corresponding flap and slat position for each configuration is shown in Table 2. Configuration 1+F is not included in Table 1 as it is commonly used for Take-off.

Table 1: Lift-to-Drag ratio for the final approach phase

Configuration	R_f
0	17.76
1	15.38
2	12.45
2+LG	9.35
3	10.96
3+LG	8.88
FULL+LG	8.32

Table 2: Flap and slat setting for A321neo

Configuration		Slats (^{0})	Flaps (^{0})
0		0	0
1	1	18	0
	1+F		10
2		22	14
3		22	21
FULL		27	35

2.2 Trajectory Definition

An approach trajectory can be defined by separating it into several descent and decelerating segments. An example of such a definition is presented in Figure 1, for a conventional approach procedure. The procedure starts from 7000 ft (or 2134 m) and a level flight with deceleration is performed (segment 1-2). This is followed by descending with a 3^o glide slope and a constant speed (segments 2-3 and 3-4) until the intermediate level flight segment is reached at 3000 ft (or 914 m). Then, a constant speed level flight segment is performed (segment 4-5) followed by an idle descent (segment 5-6) until the final approach starting point at about 1500 ft (or 457 m). The final approach (segment 6-7) is, for the most part, performed with a constant speed but in some cases a small decelerating segment exists, as indicated in Figure 1.

For the present study, the trajectories are defined through a control vector that includes three parameters for each point, from points 2 through 5. These parameters include the flight path angle, γ, which is kept constant for each individual segment, the altitude or distance to touch down of the point and the initial airspeed, V, which is either kept constant or decreases. The position and initial speed of the starting point, point 1 in Figure 1, are kept constant for all trajectories and only the flight path angle is varied. The final approach segment (6-7) is not modified for the present study as it is subject to a number of constraints, due to safety issues, and a detailed analysis and permission would be required to apply any modification to the procedure. Then, for point 5, the flight path angle is not required as it is computed in order to reach the final approach point 6. Apart from these points, the configuration changes and landing gear position are also defined. With the aforementioned input parameters and Eq. (1), all the required aircraft performance parameters can be computed.

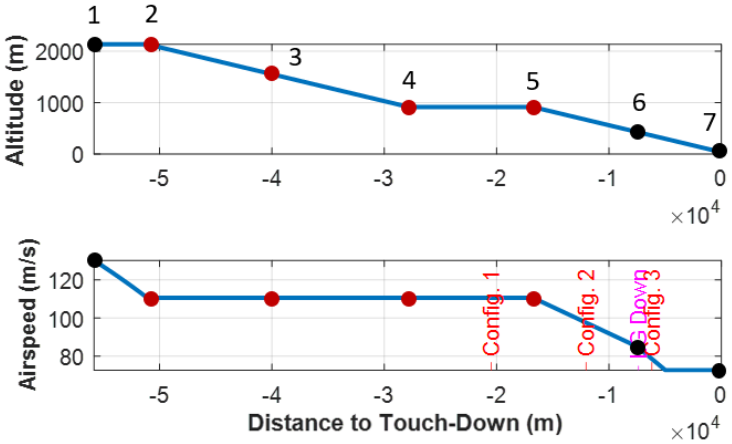

Figure 1: Conventional approach trajectory definition.

2.3 Engine Performance

Once the trajectory has been designed, the performance of the engine is evaluated using the in-house code, GESTPAN (GEneral Stationary and Transient Propulsion ANalysis) [4]. The trajectory model feeds into GESTPAN the thrust of the engine, the speed, the altitude, the temperature, the pressure, the configuration and the drag coefficient for each point along the path and several performance files are generated. These files include parameters regarding the aircraft state and the engine operating conditions and geometric characteristics, including the required parameters for the noise and emissions estimation, such as component temperatures, pressures, rotational speed and fuel consumption. They are generated for every point of the trajectory and are used to perform the noise and emissions calculations.

2.4 Noise Modelling

Aircraft noise can be classified into two categories: propulsive or engine noise and non-propulsive or airframe noise. Several prediction methods exist in each of the aforementioned categories which can be broadly identified as either theoretical or best practice methods. The difference between the two is that the former relies on physical models based on empirical or semi-empirical data while the latter relies on simple source models based on measurements (e.g. fly-over measurements). An overview of the existing methods and challenges in aircraft noise prediction is presented by Filippone [5].

Theoretical methods are currently the best option when evaluating noise along a trajectory for single flight events and, hence, for designing trajectories. In this work, empirical and semi-empirical

noise source models, implemented in the in-house noise code CHOICE (CHalmers nOIse CodE) [6], are used. The code has been described in detail and validated in [7] and has previously been used for the estimation of noise from standard trajectories and at the certification points. For this study it has been modified in order to perform noise mapping and calculate the ground noise level along the trajectory. More specifically, it has been connected with SAFT (Simulation of Atmosphere and air traFfic for a more silenT environment) [8] which is a simulation platform able to perform noise propagation calculations and contour simulations. As presented by Tengzelius et al. [9], SAFT is a tool that includes several computational methods for the prediction of noise, such as the standard ECAC Doc. 29 method, as well as more accurate simulation-based methods. However, it should be noted that these are not used for this study. Apart from the prediction of noise, one of the main functionalities in SAFT is the propagation of sound in a refractive atmosphere and the generation of noise contours on a map. CHOICE and SAFT have been linked so that the former predicts the source noise for every point along the trajectory and the latter performs the propagation and noise mapping on the ground.

2.5 Emissions Modelling

NO_x emissions are calculated based on semi-empirical models implemented in the CHEESE code (CHalmers Engine Emissions Simulation Environment). As with the noise code, CHEESE has been presented and validated in [7]. The method implemented for this study is developed by AECMA (European Association of Aerospace Industries) and is based on compressor outlet pressure and temperature, as presented in Eq. (2).

$$EI_{NO_x} = 2.0 + 28.5\sqrt{\frac{p_3}{3100}}\exp\left(\frac{T_3-825}{250}\right) \tag{2}$$

where p_3 and T_3 are the compressor outlet pressure and temperature in kPa and K respectively. EI_{NO_x} is the emissions index for NO_x and is calculated in g/kg of fuel consumed. The total NO_x mass of the procedure is simply the sum of the indices multiplied by the fuel flow for each flight segment along the trajectory.

Apart from NO_x, other emissions that have been calculated are CO_2 and SO_x. These are directly proportional to the total fuel consumption which is estimated from GESTPAN.

2.6 Optimization

Using the trajectory definition introduced in Section 2.2, a preliminary optimization is performed starting from the conventional approach trajectory definition. The control vector of the optimization process was described in the same section, but it is important to introduce some constraints regarding these parameters. These constraints concern safety requirements, operational limitations as well as path constraints. For an arriving aircraft, climbing is not allowed. Thus, the following constraint is introduced

$$\gamma \leq 0^o \tag{3}$$

Another constraint related to safety is that the flight path angle should not reach values smaller than -5^o. Therefore, the value range of γ is set to $[-5^o, 0^o]$. Furthermore. acceleration is generally not allowed during the descent segments but the aircraft might, in some cases, accelerate during a level flight segment. For the present study, it is assumed that the approach path only consists of constant speed and decelerating segments.

Finally, some speed constraints should be set for each configuration. The allowed operational speed range for each configuration is presented in Table 3, where V_0 is the initial speed at the start of the approach trajectory and V_L is the final landing speed. These values are derived from available FDR data, in combination with notes for the A321neo, [10].

The optimization problem consists of two objectives, noise and NOx emissions. For this problem, the fuel consumption was not included as an objective function. For the noise, a location was selected underneath the aircraft flight path where a small community is located. This community is found approximately 15 km from the runway threshold. Fortunately, the area around Arlanda is rather sparsely populated so the selected location only serves as an example to show the benefits of trajectory optimization. The EPNL (Effective Perceived Noise Level) metric was used for the optimization, which is a measure that is used for aircraft noise certification and indicates the relative

noise from individual aircraft. For the NO_x emissions, the total NO_x mass produced by the aircraft during the procedure was used. The two objectives are presented in Eq. (4), where the subscript *com* indicates that the EPNL is estimated at the selected community. The objectives were normalized with respect to the noise, $EPNL_{com,conv}$, and emissions, $M_{NO_x,conv}$, respectively, that are produced by the conventional approach presented in Figure 1.

Table 3: Configuration setting speed limits

Configuration	$V\ (kn)$
0	V_0 – 210
1	235 – 170
2	215 – 145
3+LG	195 – V_L

$$J_1 = \frac{EPNL_{com}}{EPNL_{com,conv}}, \quad J_2 = \frac{M_{NO_x}}{M_{NO_x,conv}} \tag{4}$$

The optimization was performed using NSGA-II, which is a nondominated sorting-based multiobjective genetic algorithm, introduced by Deb et al. [11]. This algorithm takes as input an initial value for the free parameters of the optimization, the constraints, a range within which the parameters are allowed to vary and the objective function. For the objective function, the trajectory is first generated as previously described. Then, the engine performance model is called which generates all the required performance files for the noise and emission estimates.

From the generated results, a pareto front was constructed and the optimal solution was selected using the TOPSIS (Technique for Order of Preference by Similarity to Ideal Solution) method [12]. According to this method, a utopian point and a worst point are determined relative to the set weight values for each objective function. For this study, the same weight of 0.5 was set for both objectives. The similarity of each pareto point to the worst solution is then determined, using the Euclidean distances, which are calculated from Eq.(5) and Eq.(6) for the best and worst point respectively.

$$d_{ib} = \sqrt{\sum_{j=1}^{2}\left(t_{ij} - t_{bj}\right)^2} \tag{5}$$

$$d_{iw} = \sqrt{\sum_{j=1}^{2}\left(t_{ij} - t_{wj}\right)^2} \tag{6}$$

where t_{ij} represents the weighted normalized objective, j, for the solution, i, in the pareto front.

The similarity to the worst condition is, then calculated as

$$s_{ib} = \frac{d_{iw}}{d_{iw}+d_{ib}} \tag{7}$$

The similarity can take values between 0 and 1. The higher the similarity value the better the solution.

3. Results

A number of trajectories have been generated for this study. The analysis starts from the Continuous Descent Approach (CDA) and the Low Drag Low Power (LDLP), which are the most common noise abatement trajectories. These procedures are then modified to more advanced variations to examine the possibilities of further improvement with regard to the environmental impact with small adjustments in the trajectory design. A case for a multi-level approach is also presented. This is not a common practice implemented for the purpose of noise reduction but it is one of the standard procedures used during approach. Finally, an optimized approach procedure is presented. The optimization starts from a conventional approach, which is included in the results for comparison, and the trajectory is optimized in order to minimize the noise in the specified location and the total procedure NO_x emissions as described in Section 2.6.

The generated trajectories are presented in Figure 2 through Figure 9. For all cases, the flight profile is presented along with the true airspeed, the configuration changes and the thrust. The ground path is kept constant.

During the CDA, Figure 2, as the name suggests, there are no intermediate level segments. On the contrary, the aircraft starts to descent from an altitude of about 7000 ft, with a constant descent angle of approximately 3^o. This way, the aircraft stays higher for a longer period resulting in a reduction in ground noise. During the LDLP, Figure 3, the flap extension and landing gear deployment are delayed, yielding in a decrease in drag and consequently in power requirement. In this approach, the speed is normally kept constant when the aircraft is descending and starts to decrease when a level segment is performed. For the descending segments a 3^o glide slope is used. Note that, the presented trajectories are not the only possible cases for CDA and LDLP but rather a typical representation of them.

From the CDA, two more advanced procedures are designed, the Steep CDA, Figure 4, and the Segmented CDA, Figure 5. As the name suggests, a Steep CDA is a continuous descent procedure performed with a higher descent angle. In practice, a descent with a 5^o degree angle or more might be feasible in some cases depending on the aircraft type and local weather conditions but for safety reasons it is usually avoided. A maximum angle of $4^o - 4.5^o$ is normally used. In this case, the landing configuration must be set before the aircraft starts to descent. This results in a descent with low constant speed until the final approach point is reached. Then, a 3^o angle is set and the final approach segment is performed as in a conventional procedure. The Segmented CDA includes multiple segments, with no level flight in between. The procedure starts from a normal descent with a 3^o glide slope and constant speed, transitioning into a decelerated descent with a smaller glide slope when the configurations and landing gear are deployed and, finally, into a steep descent before reaching the final approach phase.

A more advanced low drag low power procedure, Figure 6, is created by reducing the length of the intermediate level flight segment. The aircraft flies higher for a longer distance and starts to descent with idle power like in a normal LDLP. When the level flight segment is reached the airspeed is gradually reduced. The flaps and the landing gear are extended during the final descent segment of the procedure in order to avoid an increase in drag. Another approach procedure that consists of multiple segments is the Multi-level approach, Figure 7, and as the name suggests it is constructed from multiple level flight segments. Contrary to the LDLP or the Advanced LDLP, the aircraft starts the descent from 7000 ft sooner. The descent is performed with constant speed until about 5000 ft when a decelerating level flight is performed. This is followed by another descent and level flight segment until the starting point of the final approach is reached. During the descent segments the engines are set to idle but are forced to spool up during the level flight.

The trajectory definition for the Conventional approach was described in detail in Section 0 but is also presented in Figure 8, together with the power requirement. The optimized trajectory is shown in Figure 9, where the green dot indicates the microphone or community location. The vertical profile of the trajectory resembles that of a segmented CDA but the configuration changes are delayed. When overpassing the microphone, the aircraft is not flying higher compared to the Conventional approach but it is flying with a lower speed. Configuration 1 is set earlier in the Optimized trajectory while configuration 2 and higher are deployed after the aircraft overpasses the microphone. In this way, the aircraft is in steady state when it approaches the microphone and the thrust increase is avoided.

Figure 10 through Figure 17 show the corresponding noise level on the ground. For the noise mapping, the Sound Exposure Level (SEL) is used, which is an indicator of total sound energy accounting both for the received level and the duration of exposure. The total emissions from each trajectory are presented in Table 4 together with the peak SEL value and the EPNL at the location that has been selected for the noise minimization.

As it can be seen from Figure 10 and Figure 11, CDA results in higher noise level when further away from the landing point due to the higher power requirement and the earlier flap extension. As the aircraft approaches the turn, the noise from the LDLP increases which can be attributed to the lower flight altitude, the higher airspeed, the higher power requirement and the flap extension at this point. When approaching the landing point, the two procedures are very similar and there are no significant differences observed in the noise level. The peak SEL for the two procedures is presented in Table 4. This peak is observed close to the landing point and as it can be seen it is almost the same for both trajectories. Regarding the emissions, CO_2 and non-CO_2 emissions were calculated for both procedures, as presented in Table 4. It is clear that the CDA results in higher emissions and fuel consumption, which was expected as the LDLP is designed for lower power requirement.

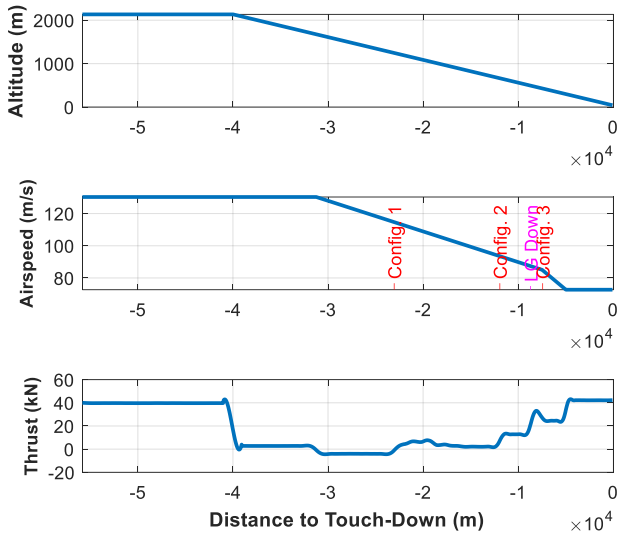

Figure 2: Flight profile and performance for a CDA

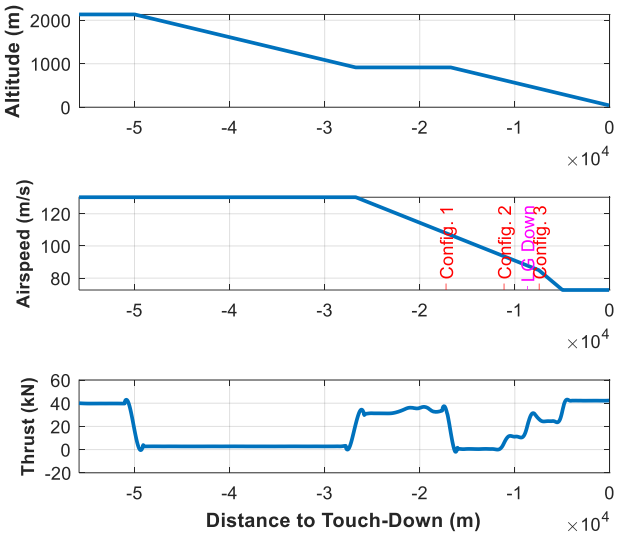

Figure 3: Flight profile and performance for a LDLP

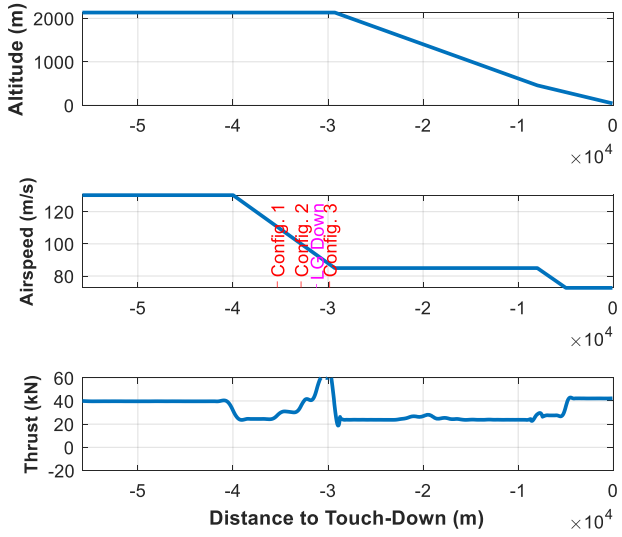

Figure 4: Flight profile and performance for a Steep CDA

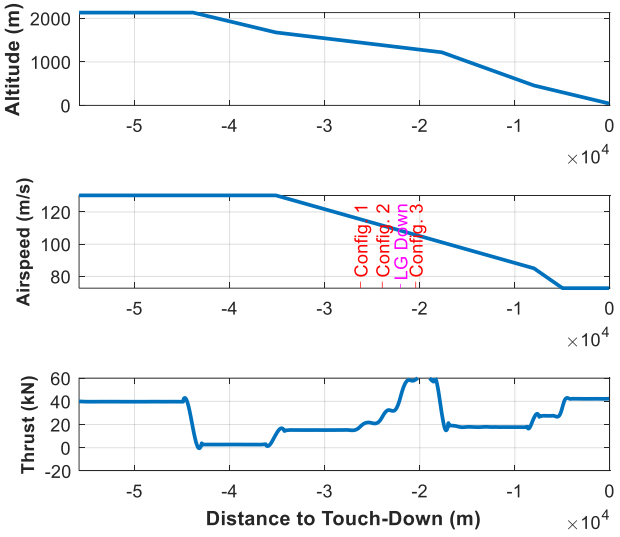

Figure 5: Flight profile and performance for a Segmented CDA

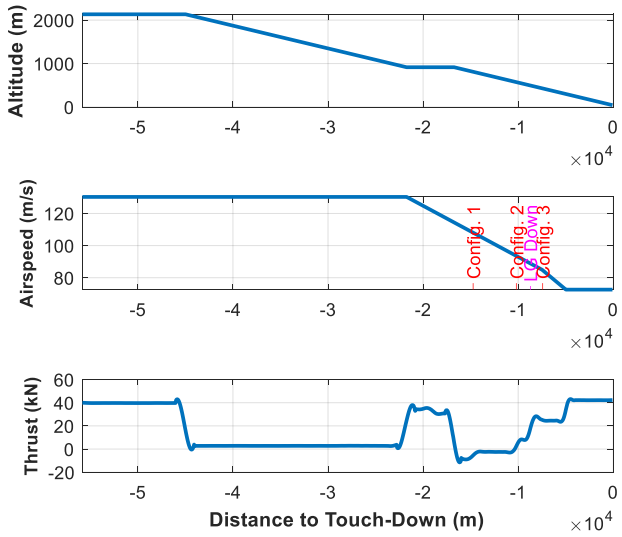

Figure 6: Flight profile and performance for an Advanced LDLP

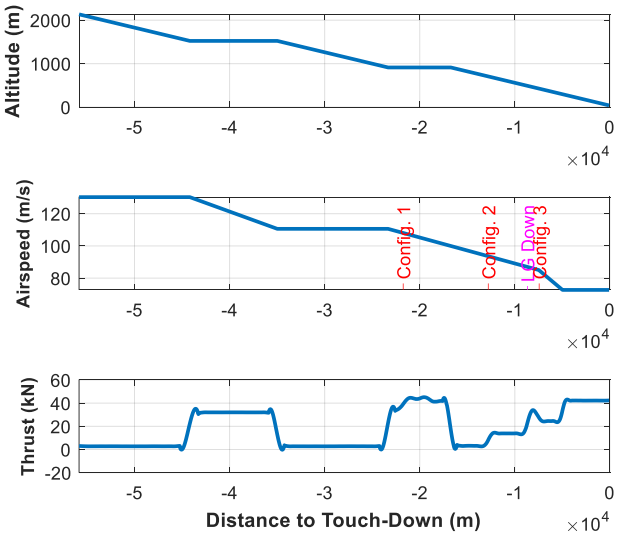

Figure 7: Flight profile and performance for a Multi-level approach

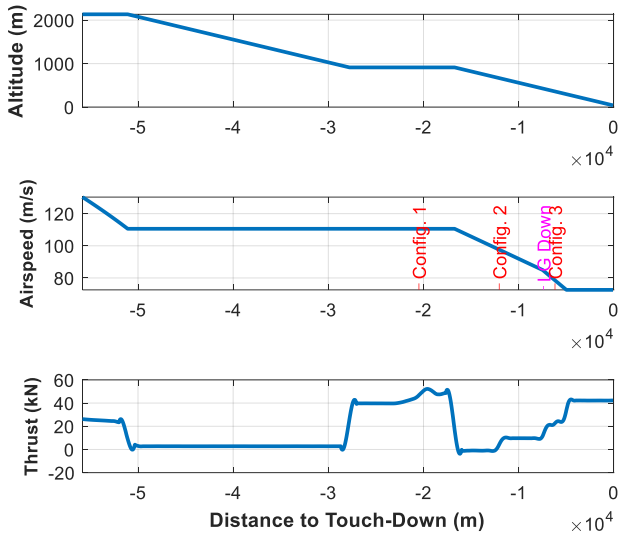

Figure 8: Flight profile and performance for a Conventional approach

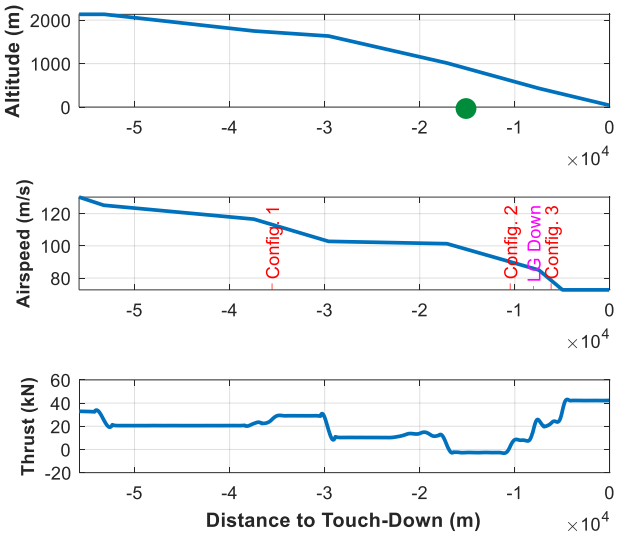

Figure 9: Flight profile and performance for the Optimized approach

Compared to the CDA, the Steep CDA, Figure 12, does not seem to result in any improvement in the SEL contour. Even though the aircraft stays higher for longer, the increase in drag and thrust due to the early flap deflection cause an increase in noise level. The 80 and 85 dB contour areas are significantly increased and so are the emissions, Table 4. When compared with the LDLP, an improvement is observed in the turn area, however this is again counteracted with increased emissions. Improvement is also observed in the peak SEL which occurs close to the landing point. In the case of the Steep CDA, the aircraft is already in steady state when approaching the landing point and, thus, less noise is generated.

Regarding the Segmented CDA, Figure 13, some noise reduction is achieved further out from the airport, where the initial decent point is located. The 75 and 80 dB contours are decreased at this point compared to the CDA. However, an increase is observed after this point when the second segment is reached. Compared to the LDLP, there seems to be no benefit regarding the noise level, with the exception of a small region before the second segment of the Segmented CDA is reached. During the turn, the high noise level generated from the Segmented CDA is attributed to the consecutive configuration changes and the change in glide slope which increase the drag and cause the engine to spool up. An improvement is again observed closer to the airport as the maximum SEL does not exceed 98 dB. The emissions from this procedure are significantly higher than the CDA and LDLP but remain less than the Steep CDA operation. It is evident that these procedures are to be used only when noise reduction close to the landing point is required but even in this case the increase in emissions should not be neglected.

In Figure 14, the SEL contour for the Advanced LDLP is presented. The 75 dB contour is slightly reduced compared to the LDLP, Figure 11, but the reduction in the 80 and 85 dB areas is evident. In both cases, the increase to 85 dB occurs during the intermediate level flight segment which explains the reduction for the Advanced LDLP (shorter level flight segment). Interestingly, the CO_2 and SO_x emissions are slightly decreased but an increase is observed in the total NO_x mass, Table 4. Even though the initial level flight segment, which requires higher engine power, is longer the engine thrust increase in the intermediate level flight segment is shorter in the Advanced LDLP and the whole procedure requires less time due to the higher speed which explains the reduced fuel consumption. Contrary to CO_2 and SO_x, NO_x emissions also depend on the atmospheric conditions and altitude. Furthermore, the aircraft flies at a higher airspeed for longer causing the engine to throttle up which causes an increase in the compressor outlet temperature and pressure and, hence, the NO_x emissions.

Regarding the Multi-level approach, Figure 15, the increase in noise is notable during the level flight segments which is explained by the thrust increase. When compared with the CDA, Figure 10, it does not seem to result in any improvement with the exception of a few points, before the turn, in the 75 dB contour area. In this case, there is a decrease in total NO_x mass as the aircraft flies with lower speed overall, but the intermediate level flight segment in combination with the increased flight time result in a slight increase in fuel consumption. In comparison to the LDLP, the Multi-level results in higher noise level further out from the airport, caused by the first level flight segment, but some

improvement is observed closer to the turn. The 85 dB contour area is smaller in this case as the second level flight segment is kept shorter and the airspeed lower, compared to the segment of the LDLP at this location. Configurations 1 and 2 are set earlier for the Multi-level approach which results in increased noise closer to the airport, as can also be seen from the peak SEL value. The emissions are fairly similar with a slight decrease in NO_x and an increase in CO_2 and SO_x which can partly be attributed to the lower overall speed for the former and the higher drag and power requirement due to the earlier flap extension and the increased flight time for the latter.

The SEL contour for the Conventional approach, Figure 16, looks very similar to the one for the LDLP. Surprisingly, a decrease in noise level is observed further out in the flight path as the 80 dB contour area evidently decreases. On the other hand, the 85 dB area closer to the airport and at the turn is slightly increased. The emissions and peak SEL are almost the same, with a minor increase in fuel flow for the Conventional approach.

The optimized trajectory, Figure 17, evidently results in significant improvement in the SEL contour, not only compared to the Conventional approach but with most of the examined trajectories. Despite the increase in the 80 dB contour area, the 85 dB area is the smallest from all the trajectories and only appears close to the landing point. In the area around the community (indicated with the black square in the figure) the noise level goes down to 75 dB, which is explained by the lower speed and steady state of the aircraft. NO_x emissions show a notable reduction compared with the rest of the trajectories. The fuel consumption indicates a minor increase but it is not considered important compared to the achieved reduction in NO_x and noise. The increase can be explained by the somewhat increased flight time and by the fact that the engine is not set to idle for a large part of the procedure. As expected, the EPNL at the microphone has the lowest value and is reduced by more than 2 dB, compared to the Conventional approach. A reduction can also be noticed in the peak SEL value.

Table 4: Environmental trades for each trajectory

Trajectory	Duration (sec)	NO_x (kg)	CO_2 (kg)	SO_x (kg)	Peak SEL (dB)	EPNL (dB)
CDA	512	2.02	726.47	0.19	106.4	74.5
LDLP	505	1.87	702.76	0.19	106.1	74.9
Steep CDA	580	2.90	1188.89	0.32	97.3	79.4
Segmented CDA	521	2.75	969.39	0.26	97.6	80.8
Advanced LDLP	496	1.95	691.04	0.18	105.6	74.2
Multi-level	534	1.83	749.83	0.20	107.3	74.6
Conventional	545	1.84	723.90	0.19	106.9	75.3
Optimized	548	1.60	757.18	0.20	97.2	73.1

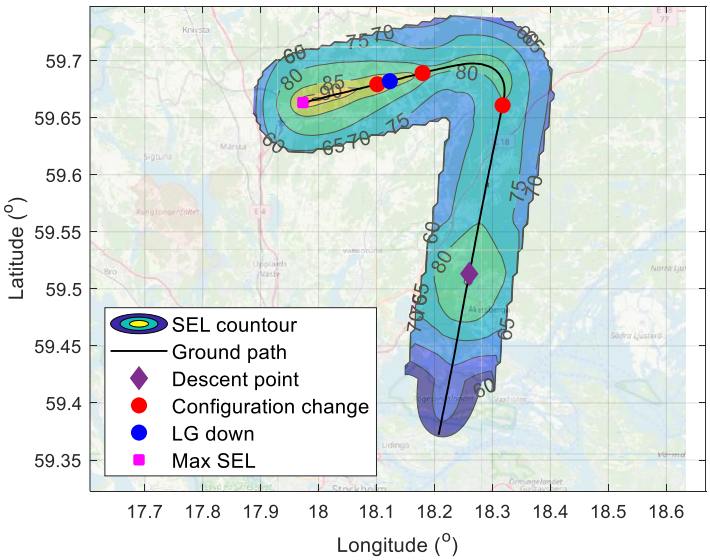

Figure 10: SEL contour for a CDA

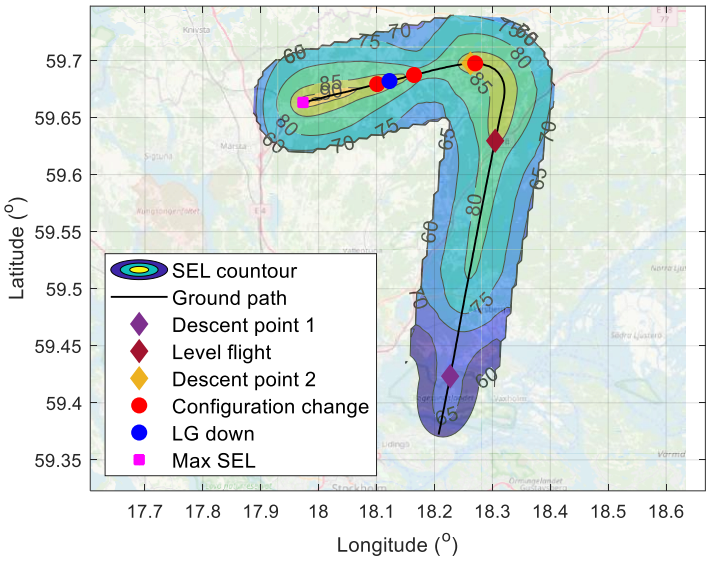

Figure 11: SEL contour for a LDLP

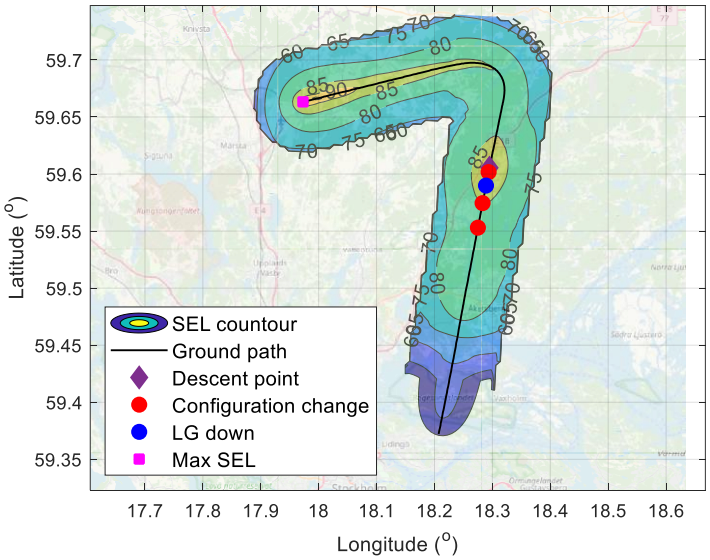

Figure 12: SEL contour for a steep CDA

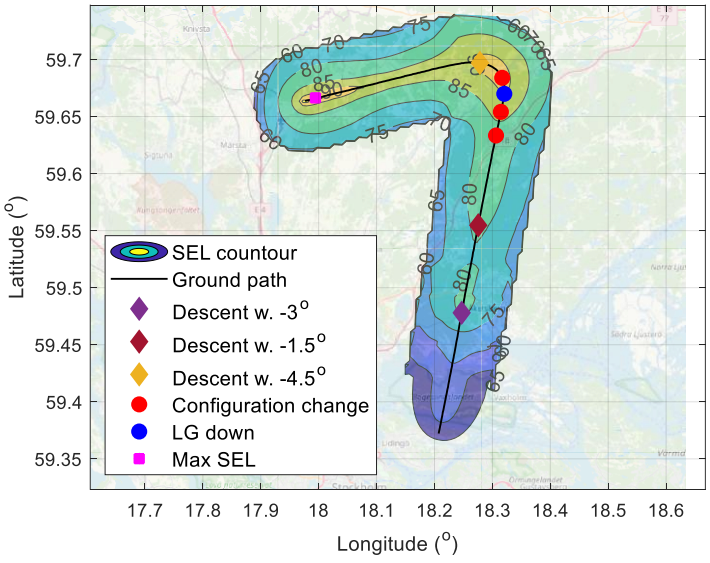

Figure 13: SEL contour for a segmented CDA

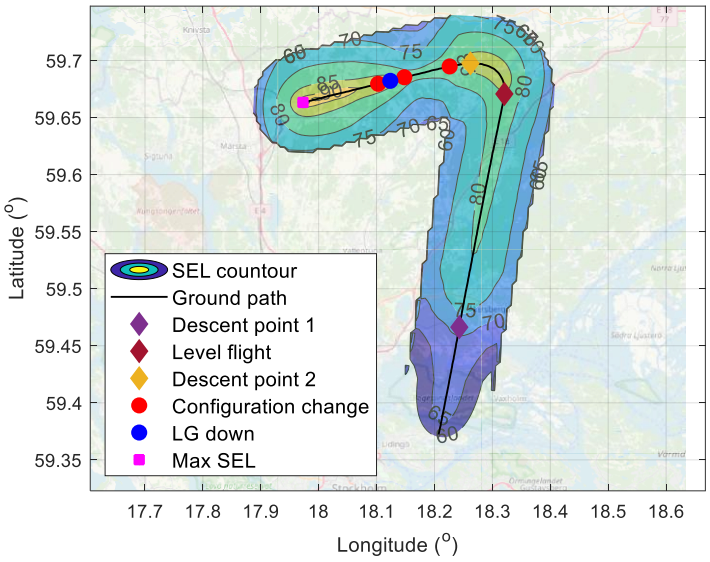

Figure 14: SEL contour for an advanced LDLP

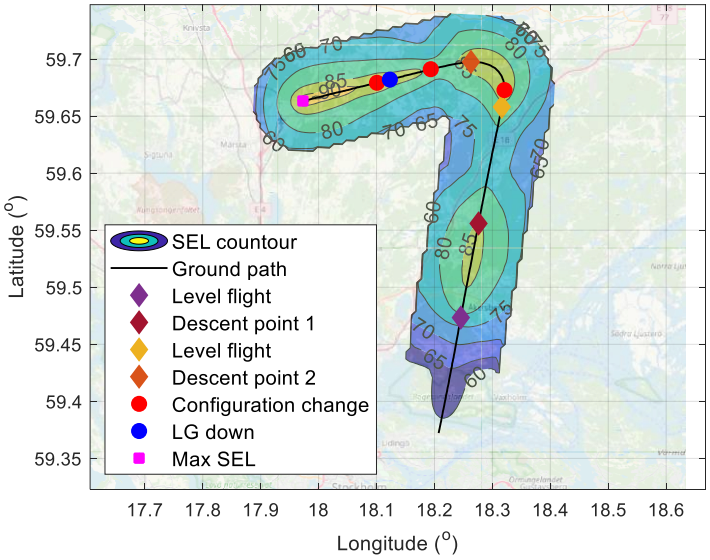

Figure 15: SEL contour for a multi-level approach

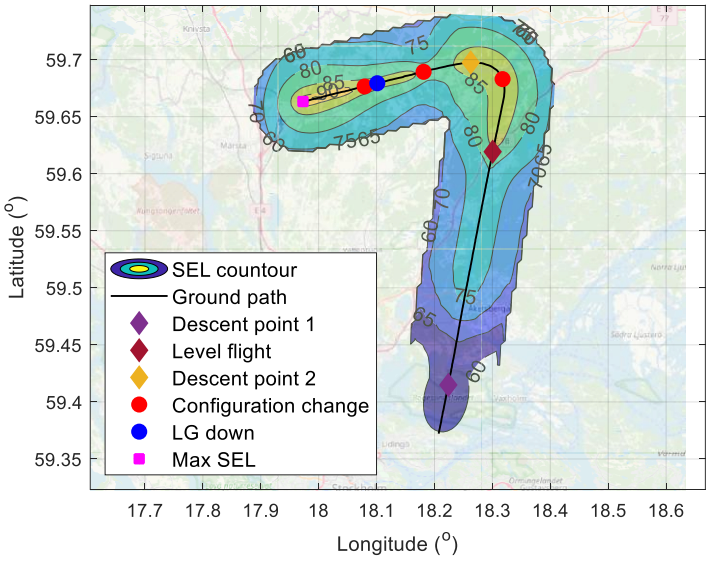

Figure 16: SEL contour for a conventional approach

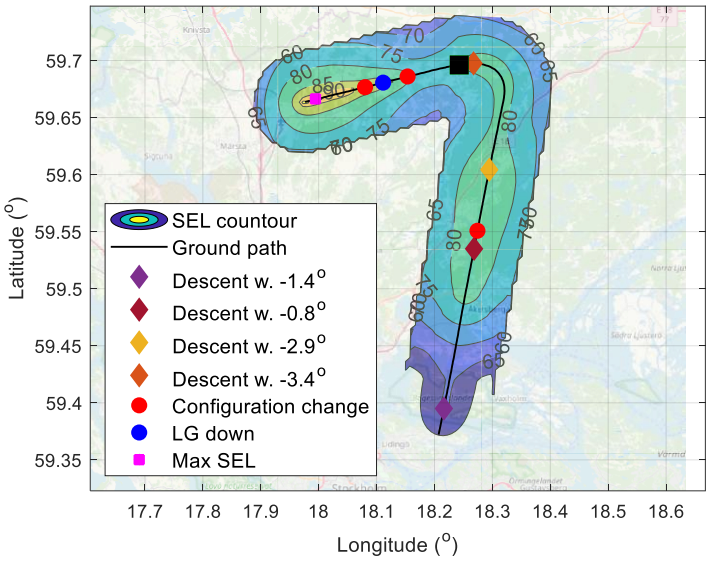

Figure 17: SEL contour for the optimized approach

4. Conclusions

In this study, several approach trajectories are evaluated for noise and emissions. The comparison indicated that the results are strongly affected by the flight parameters. It is not possible to say if one of them is generally better as this depends on the airport, flight conditions, atmospheric conditions and the aircraft type. For example, if the aim was to reduce the noise disturbance for a community located further away from the airport, the LDLP or the Advanced LDLP would be a better option than the CDA. On the other hand, in that region the aircraft flies higher and it is usually closer to the airport that the increased disturbance occurs. In that case, CDA or even the Steep CDA and the Segmented CDA are a better solution. The Multi-level approach could be used with adjustments when noise reduction in specific locations is required. When looking at the emissions, in terms of CO_2, SO_x and NO_x, it is evident that both the LDLP and the Advanced LDLP have an advantage, however the difference is not that significant from the Multi-level and the CDA, indicating that emissions could be traded for noise depending on the desired noise reduction. Observing all the generated SEL contours, one general conclusion that can be drawn is that in most cases, noise reduction in proximity to the airport results in increased noise further away. It was also shown that the more advanced the trajectory is, the higher is the increase in NO_x emissions but not necessarily in fuel consumption.

As it was mentioned earlier, contrary to CO_2 and SO_x, NO_x will also depend on the climate and local weather conditions and it could differ from the values presented here. This becomes apparent by observing Eq. (2). Both the temperature and the pressure from the compressor depend on the atmospheric properties and the aircraft speed, which could explain the opposite trend variation compared to the other emissions in some cases. Weather could also have an effect on the propagation of noise, especially if strong wind is present. However, it is not within the scope of this study to account for these effects.

The optimization, evidently, resulted in the best solution for the selected scenario. Despite aiming to minimize the noise at a specific location, the SEL contour showed some improvement compared to other trajectories. As expected, the decrease in noise closer to the airport resulted in an increase further away. Even though the total NO_x mass was significantly improved, the CO_2 and SO_x emissions indicated a slight increase. This is not a surprise since the fuel consumption was not included in the objective function. If the optimization accounted for the fuel flow, an improvement in all three parameters could have been achieved, however it is very likely that the reduction in noise and NO_x emissions would not have been that significant.

It becomes apparent that designing trajectories is a complex matter that requires extensive analysis and adaptation to different conditions. It is important to account for several factors, from noise assessment to fuel efficiency to pilot workload. Here the focus was directed on the environmental impact of the procedures and evaluating trade-offs between noise and emissions. Although, it was shown that the standard noise abatement approach trajectories may result in good trades between noise and emissions, there is no doubt that for specific scenarios, trajectory optimization is the best option.

5. Acknowledgements

This research was funded by the Centre for Sustainable Aviation (CSA) at KTH Royal Institute of Technology, Stockholm, Sweden in cooperation with the Swedish Transport Administration, Trafikverket.

6. References

[1] R. Koenig and O. Macke, "Evaluation of simulator and flight tested noise abatement approach procedures," in *26th International Congress of the Aeronautical Sciences*, Braunschweig, Germany, 2008.

[2] Environmental Research and Consultancy Department, "Review of Arrival Noise Controls," Civil Aviation Authority, West Sussex, 2017.

[3] P. M. A. De Jong, Continuous Descent Operations Using Energy Principles, Ede, The Netherlands: GVO drukkers & vormgevers B.V. , 2007.

[4] T. Grönstedt, "Development of methods for analysis and optimiztaion of complex jet engine systems," Gothenburg, 2000.

[5] A. Filippone, "Aircraft noise prediction," *Progress in Aerospace Sciences,* vol. 68, pp. 27-63, 2014.

[6] L. Ellbrant and D. Karlson, "A Noise Prediction Tool for Subsonic Aircraft and Engines including a NumericalInvestigation of Noise Radiation," Gothenburg, 2008.

[7] E. M. Thoma, T. Grönstedt and X. Zhao, "Quantifying the Environmental Design Trades for a State-of-the-Art Turbofan Engine," *Aerospace,* vol. 7, no. 148, 2020.

[8] "SAFT," Centre of Sustainable Aviation, 11 11 2020. [Online]. Available: https://www.kth.se/csa/projekt/avslutade-projekt/saft-1.991973.

[9] U. Tengzelius, A. Johansson, M. Åbom and K. Bolin, "Next generation aircraft noise-mapping," in *Inter-noise*, Washington, DC, 2021.

[10] E. Parks, "Airbus Notes: Training Notes for A319/320/321," 2022.

[11] K. Deb, A. Pratap, S. Agarwal and T. Meyarivan, "A Fast and Elitist Multiobjective Genetic Algorithm: NSGA-II," *IEEE Transactions on Evolutionary Computation,* vol. 6, no. 2, pp. 182-197, 2002.

[12] B. Uzun, M. Taiwo, A. Syidanova and D. Uzun Ozsahin, "The Technique For Order of Preference by Similarity to Ideal Solution (TOPSIS)," in *Application of Multi-Criteria Decision Analysis in Environmental and Civil Engineering*, Cham, Switzerland , Springer, 2021, pp. 25-30.

Copyright Statement